Gas-Phase ^{1}H NMR Studies of Internal Rotation Barriers and Conformer Stabilities of *N*-Ethyl, *N*-Methylthioamides

Angela N. Taha, Susan M. Neugebauer-Crawford,† and Nancy S. True*

Chemistry Department, University of California, Davis, California 95616

Received: April 4, 2000; In Final Form: June 13, 2000

Kinetic parameters and conformational equilibrium constants characterizing the internal rotation in gaseous *N*-ethyl, *N*-methylthioformamide (EMSF), *N*-ethyl, *N*-methylthioacetamide (EMSA), and *N*-ethyl, *N*-methyltrifluorothioacetamide (EMSTFA) are determined from exchange broadened ^{1}H NMR spectra. The $\Delta G^{\ddagger}_{298}$ values, in kcal mol^{-1}, are 22.6 (0.1), 17.8 (0.1), and 17.2(0.1) for EMSF, EMSA, and EMSTFA, respectively. Conformer Gibbs free energy differences, $\Delta G°$ ($\Delta G° = G°$ (methyl group syn to thionyl sulfur) $-$ G° (methyl group anti to thionyl sulfur)), in cal mol^{-1}, are -123 (24), 56 (9), and 96 (13) for EMSF, EMSA, and EMSTFA, respectively. These results are compared to solution phase values and to the corresponding oxoamides.

Introduction

The conformations of amides have been the subject of substantial investigation in the past.[1−9] More recently, studies have been extended to thioamides[10−18] in an effort to understand the similarities and differences between these two classes of molecules. It is well know that amides have an extremely important role in the activity and function of biologically important systems. According to the simple resonance model, the stability of the amide framework is the result of the partial double bond character of the C−N bond.[3] The resonance model has been quite successful in describing and predicting effects of nitrogen and carbonyl substitution on the magnitude of the rotational barriers.[1−9] In general, carbonyl substituents larger than hydrogen lower the rotational barrier due to an unfavorable steric interaction with the nitrogen substitutuents which causes destabilization of the planar ground state. The electronegativity of the substituent attached to the carbonyl carbon also has a marked effect on the magnitude of the rotational barrier. In general, increasing the substituent's electronegativity increases the barrier. A recent gas-phase study from our group reported that thiocarbonyl carbon substitution in *N*,*N*-dimethylthioamides also results in large changes in the rotational barrier.[18] Again, as in the oxoamides, increasing substituent size decreases the barrier and increasing the substituent electronegativity increases the barrier. The effects, however, are more pronounced in thioamides than in the corresponding oxoamides. The present study investigates the dependence of the rotational barrier height on substitution at the thiocarbonyl carbon in *N*-ethyl, *N*-methylthioamides.

Asymmetric amides exist as mixtures of conformational isomers. For dialkyl substituted asymmetric amides, the conformational equilibrium is primarily determined by steric interactions. Previously reported solution phase and gas-phase studies of *N*-methyl, *N*-alkyl asymmetric amides investigated the conformational preference with changing size of the *N*-alkyl substituent.[1,5,6] Substituents ranged from ethyl to *tert*-butyl groups. The studies showed that the preferred configurations of formamides have the *N*-methyl group syn to the carbonyl oxygen. This configuration minimizes steric repulsion between the carbonyl oxygen and the more bulky nitrogen substituent. For the trifluoroacetamides and acetamides, the preferred configuration has the *N*-methyl group anti to the carbonyl oxygen. In this case the interaction between the CF_3 or CH_3 group and the *N*-alkyl substituent is minimized.

This study examines the Gibbs free energy differences, $\Delta G°$ and $\Delta G^{\ddagger}$, characterizing the internal rotation of gaseous and solution phase *N*-ethyl, *N*-methylthioformamide (EMSF), *N*-ethyl, *N*-methyltrifluorothioacetamide (EMSTFA), and *N*-ethyl, *N*-methylthioacetamide (EMSA). This is the first study of asymmetrically substituted thioamides. The results are compared to the corresponding oxoamides. It is expected that thionylation will have significant effects on the $\Delta G^{\ddagger}$ values as seen with *N*,*N*-dimethylthioamides which have barrier heights ca. 2 kcal mol^{-1} higher than the corresponding *N*,*N*-dimethylamides. The origin of the increased barrier heights has been at the center of controversy for several years. Several studies have proposed alternatives to the simple resonance model. Theoretical studies by Laidig and Cameron[12] predict a greater stabilization of the ground state structure caused by greater charge donation to the amido group from the more polarizable thiocarbonyl group. This results in a more costly rehybridization of nitrogen necessary for internal rotation in thioamides. Another model by Wiberg[11] et al. predicts a greater charge-transfer mechanism from the nitrogen to sulfur compared to nitrogen to oxygen. This increased ability to donate charge to the sulfur atom is the result of the small electronegativity difference between the sulfur and carbon atoms and the larger size of the sulfur atom. However, an *ab initio* valence bond study recently reported that resonance effects are more important in thioformamide than in formamide, with conjugation effects accounting for two-thirds of the rotational barrier of thioformamide compared to one-third for formamide.[15] It has been shown by a previous experimental report from our group[18] that models predicted by Wiberg et al. and Laidig and Cameron both adequately describe the barrier height increase in most cases. This study reported that the simple resonance model does not adequately predict the experimental trends.

† Current address: Department of Chemistry, California State University, Sacramento, California 95819.

10.1021/jp001297q CCC: $19.00
Published on Web 07/26/2000

Variable-temperature NMR methods allow for the elucidation of the temperature dependence of interconversion rate constants and conformer populations to yield a complete set of kinetic and thermodynamic parameters. Effects of solvation will reflect the stabilizing or destabilizing role of solvent perturbations on the $\Delta G°$ and $\Delta G^{‡}$ values. It has been well established that amide self-association, amide-solvent association, solvent polarity, and amide concentration affect reaction rate.[19] We have, therefore, examined 1 mol % thioamide solutions in relatively nonpolar solvents. It has also been suggested that solvation can mask the intrinsic influence of substituents. Gas-phase studies allow for analysis of isolated molecules yielding intrinsic molecular information. They have the added benefit of providing data which can be directly compared to theoretical predictions that typically examine isolated molecules.

Experimental Section

Synthesis of *N*-Ethyl, *N*-Methylthioformamide. *N*-Ethyl, *N*-methylformamide (EMF) carbonyl precursor was prepared by aminolysis of ethyl formate (Aldrich, 0.2 mol) with *N*-ethylmethylamine (Aldrich, 0.1 mol) in ethanol at 0 °C. The reaction mixture was then allowed to slowly warm to room temperature and was subsequently refluxed for 1 h and stirred overnight. Fractional distillation yielded the oxoamide product which was then converted to the thio analogue by adding a 0.25 molar ratio of phosphorus pentasulfide (Acros Chemical) dissolved in hot xylene. The mixture was stirred with heat for 2 h. The resulting reaction mixture was filtered and washed with water and ether. The xylene was removed to yield *N*-ethyl,*N*-methylthioformamide (EMSF).[20]

Synthesis of *N*-Ethyl, *N*-Methyltrifluorothioacetamide. The carbonyl precursor, *N*-ethyl, *N*-methyltrifluoroacetamide (EMTFA) was prepared by slow addition of a molar excess of trifluoroacetic anhydride (Aldrich) to *N*-ethylmethylamine at 0 °C. The resulting mixture was washed with saturated aqueous sodium bicarbonate and extracted into diethyl ether. Removal of the ether yielded the oxoamide product which was then converted to the thio analogue by addition of phosphorus pentasulfide into room-temperature xylene. Filtration, washing with water and extraction into ether, and removal of the solvent yielded *N*-ethyl, *N*-methyltrifluorothioacetamide (EMSTFA).[20]

Synthesis of *N*-Ethyl, *N*-Methylthioacetamide. The carbonyl precursor, *N*-ethyl, *N*-methylacetamide (EMA) was synthesized by addition of acetyl chloride (Aldrich) to *N*-ethylmethylamine in CH_2Cl_2 (Aldrich). The reaction mixture was stirred for 1 h and then extracted into 1% sulfuric acid, 4% sodium bicarbonate, and saturated NaCl. Removal of the solvent yielded the amide which was then converted to the thio analogue by slow addition of phosphorus pentasulfide in warm xylene. The reaction mixture was stirred for 1 h and then filtered and washed with water to ether to yield *N*-ethyl, *N*-methylthioacetamide (EMSA).[20]

All pure liquid amides were characterized by ^{1}H NMR spectroscopy. The purity of the samples was determined on the basis of no extra resonances in the spectra.

Sample Preparation. Gas-phase NMR samples were prepared in restricted volume NMR tubes constructed from 3-cm long sections of Wilmad high-precision 12 mm coaxial inserts. The short tubes were inserted into longer 12 mm tubes for introduction into the probe. Samples were prepared by deposition of a small drop of the sample in the bottom of the sample tube. To the slightly cooled sample tube 25−40 Torr of tetramethylsilane (frequency and resolution reference) and 300−400 Torr argon (to inhibit oxidation of the samples were added). The argon partial pressures used also ensure that the rate constants obtained are in the high-pressure limit and can be analyzed using transition state theory. The tubes were torch sealed and immersed in liquid nitrogen. Samples were run from low to high temperature to avoid condensation on the walls of the insert tube.

Solution-phase NMR samples were prepared in 5 mm o.d. Wilmad NMR tubes and contained 1 mol % amide in tetrachloroethane-d_2 (EMSTFA, Aldrich) or in decalin (EMSF and EMSA, Fisher). Solvents were chosen based on relative nonpolarity and boiling point temperatures. The decalin proton resonances did not interfere with the sample proton resonances. Investigation of 0.1 mol % solutions showed the same chemical shifts and temperature dependence of the chemical shifts, indicating complete solvation at 1 mol %. All liquid samples also contained a drop of TMS as a frequency and resolution reference.

Spectroscopy. Gas-phase ^{1}H NMR spectra were acquired with a wide-bore GE NT-300 spectrometer (proton observation at 300.07 MHz) fitted with a Tecmag acquisition upgrade and equipped with a Bradley 12-mm proton probe. Liquid phase ^{1}H NMR spectra were also acquired on this spectrometer, but with a Bradley 5 mm proton probe. All measurements were made on spinning samples in unlocked mode. The spectrometer's field drift rate is negligible compared to the average spectral acquisition time. Acquisition parameters were as follows: pulse length, 14 μs (90° flip angle); delay time, 1.3 s; and acquisition time 1.638 s. No changes in the population ratios were observed for gas-phase sample acquisitions with a 5 s delay time. Delay times for liquid spectra were 10 s. Typically 4000−8000 transients were collected for the gaseous samples and 16 for the solution samples and stored in 8 K memory to achieve a maximum signal-to-noise ratio of 10:1 and 100:1 after multiplication by an exponential line-broadening factor of 1 Hz. Sweep width was ±2500 Hz, giving a digital resolution of 0.6 Hz/point. Temperatures were controlled with a 0.1 °C pyrometer and read after each acquisition. Temperature measurements for the gas-phase spectra were made using two copper−constantan thermocouples placed within an empty 3-cm long, 12 mm o.d. insert tube fitted within a 12 mm NMR tube. The temperature gradient was found to be less than 0.2 K within the active volume. Samples were allowed to thermally equilibrate for 10 min prior to sample acquisition. Solution temperatures were similarly measured, except that a single 5 mm NMR tube containing the solvent and one copper−constantan thermocouple was employed.

Parameter Determination. Rate constants were calculated for exchanging spectra by using the computer program DNMR5,[21] which uses an iterative nonlinear least squares regression analysis to obtain the best fit of the experimental spectrum. The program was provided with anti and syn proton chemical shifts at the limit of slow exchange, coupling constants, transverse relaxation times, and the digitized NMR spectrum. The temperature dependent conformer populations, extrapolated from slow exchange intensity measurements, were also input into the simulations. The effective line-width parameter was measured at slow and fast exchange for each amide system (except for gas and solution EMSF due to spectrometer temperature limitations). For these systems the effective line width parameter was measured only at a series of slow exchange temperatures. The effective line width was estimated at each temperature assuming a linear temperature dependence. The line width of TMS at each exchange temperature was used to estimate the magnetic field inhomogeneity contribution to the

TABLE 1: Rate Constants (k) for Internal Rotation in Gaseous and Solution Phase EMSF[a], EMSA[a], and EMSTFA[b] as a Function of Temperature

EMSF k (s^{-1})			EMSA k (s^{-1})			EMSTFA k (s^{-1})		
T (K)	gas	solution	T (K)	gas	solution	T (K)	gas	solution
422.6	13.4(0.4)		347.2	13.8(0.3)		315.3	6.9(0.4)	
424.5	13.5(0.4)		349.7	18.9(0.5)		317.1	7.5(0.5)	
426.6	16.3(0.3)		351.3	38.0(0.4)		319.3	11.1(0.4)	
430.2	20.8(0.4)		355.2	43.1(0.3)		321.2	12.6(0.5)	
432.7	24.3(0.2)		355.9	48.1(0.3)		323.1	15.3(0.3)	
433.1		10.8(0.4)	357.5	53.7(0.4)		325.0	17.7(0.4)	
433.6	28.5(0.2)		360.5	64.2(0.3)		327.1	19.1(0.3)	
434.6		12.1(0.2)	362.9	72.1(0.3)		328.5	22.6(0.2)	
435.5	29.6(0.2)	13.7(0.5)	364.5	95.0(1.1)		365.0		16.3(0.3)
436.9		14.3(0.2)	396.9		14.2(0.7)	366.9		18.5(0.5)
437.7	32.1(0.1)		399.2		18.3(0.9)	369.3		20.6(0.4)
438.1		16.3(0.4)	402.5		24.7(1.0)	372.8		27.5(0.9)
439.8	34.5(0.2)	18.2(0.3)	405.6		29.3(0.4)	375.4		30.6(1.2)
440.6	40.2(0.2)	20.0(0.3)	408.2		40.3(1.6)	378.1		40.3(0.8)
442.6	44.9(0.3)		412.5		49.3(1.5)	379.5		45.9(1.7)
442.8		21.5(0.2)	415.9		57.2(2.1)			
443.7		23.1(0.5)	417.5		66.8(1.7)			
444.9		25.2(0.4)	420.1		78.3(2.2)			
			422.9		99.7(3.1)			
			426.5		121.2(2.9)			

[a] Solutions of amide in decalin. [b] Solution of amide in TClE.

line width. This factor and the exponential line broadening factor were added to the interpolated values for the effective line width to obtain a total line broadening, and thus the effective transverse relaxation time (T_2) was determined at each temperature. Rate constants in the exchange region were obtained by iterating on rate constant, spectral origin, baseline height, and baseline tilt. All other parameters were held constant.

Conformer Gibbs energy differences, $\Delta G°$, ($\Delta G° = G°$ (methyl group syn to thionyl sulfur) $- G°$ (methyl group anti to thionyl sulfur)) were calculated through extrapolation of $\Delta H°$ and $\Delta S°$ from the slope and intercept of $1/T$ versus ln K_{eq}. The $\Delta G°$ values are reported at 298 K. Population ratio changes in the slow exchange region allowed for the determination of K_{eq} as a function of temperature. All populations were determined by averaging 20 integrations. Gas-phase slow exchange population ratios, p_{syn}/p_{anti}, ranged from 1.21(2) to 1.29(1) for EMSF; 0.85(3) to 0.90(2) for EMSTFA; and 0.91(1) to 0.93(0) for EMSA.

Calculations of molecular geometries and NMR shielding parameters were performed using the Gaussian 98 software package.[22] Full geometry optimizations of the syn and anti equilibrium structures were performed at the HF/6-311++G** level of theory. Vibrational frequency calculations of the structures were done to verify the minimum energy configuration. Zero-point and thermal energy corrections were evaluated using the HF/6-311++G** harmonic frequencies at 298 K and 1 atm. The calculated frequencies were scaled by the conventional factor of 0.893.[23,24] DFT calculations of the magnetic properties used the B3LYP hybrid density functional and the 6-311++G** basis. The NMR calculations employed the GIAO procedure that was recently shown to yield the most accurate chemical shielding values for a series of organic molecules used in conjunction with the B3LYP model.[25]

Results

Rate constants used to determine the gas phase and solution phase kinetic parameters from exchange broadened NMR spectra appear in Table 1. Figure 1 shows the temperature dependence of these rate constants in the form of Eyring plots. The experimental and calculated conformer Gibbs energy differences

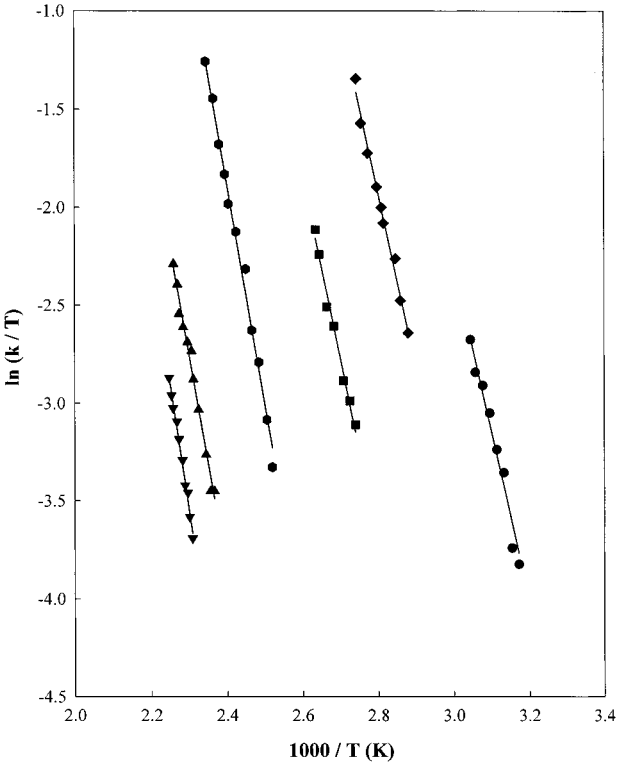

Figure 1. Eyring plots of gas and solution phase exchange rate constants for EMSF, EMSTFA, and EMSA. EMSF gas (▲), EMSF solution (▼), EMSTFA gas (●), EMSTFA solution (■), EMSA gas (◆), and EMSA solution (⬣).

at 298 K are shown in Table 2. Table 3 lists the gas and solution phase activation parameters. Spectral assignment of the conformers is described below followed by results of the exchange broadened dynamic line shape analyses.

Gas and solution phase conformational equilibrium constants were obtained by analysis of the slow exchange spectra. The slow exchange ^{1}H NMR spectra of all thioamide systems studied show both conformational forms: syn (*N*-methyl group syn to the carbonyl oxygen) and anti (*N*-methyl group anti to the carbonyl oxygen). Observation of two separate *N*-alkyl reso-

TABLE 2: Experimental and Calculated[a](HF/6-311++G) Conformer Gibbs Energy Differences ($\Delta G^\circ = G^\circ$(methyl group syn to thionyl sulfur) $- G^\circ$(methyl group anti to thionyl sulfur)) at 298 K[b]**

					dipole moment	
	ΔG°_{gas}	ΔG°_{calc}	ΔG°_{liq}	solvent	syn	anti
EMSF	−123(24)	−156	−178(10)	Decalin	5.97	5.73
EMSA	56(9)	42	30(12)	Decalin	5.92	5.72
EMSTFA	96(13)	70	56(8)	TClE-d_2	5.49	5.33
EMF[d]	−78(11)	−122	−235(8)	DMSO-d_6	4.46	4.44
EMA[d]	178(136)	128	35(6)	DMSO-d_6	4.26	4.21
EMTFA[d]	204(49)	142	27(25)	CCl_4	4.69	4.58

[a] ZPE corrections scaled by 0.8929. Energies include ZPE and thermal energy corrections. [b] ΔG° values in cal mol^{-1}. [c]Gas-phase dipole moments calculated at HF/6-311++G** level of theory. [d] Reference 5.

TABLE 3: Internal Rotation Activation Parameters for Asymmetrically Substituted Thio and Oxo[a]Amides

	$\Delta G^{\neq}_{298}$		$\Delta H^{\neq}$		$\Delta S^{\neq}$	
	gas	liquid	gas	liquid	gas	liquid
EMSF	22.6(0.1)	24.3(0.1)	22.0(1.8)	25.9(1.5)	−1.9(4.2)	5.4(3.0)
EMSA	17.8(0.1)	21.6(0.1)	18.1(0.3)	22.5(1.2)	1.0(0.3)	3.1(2.1)
EMSTFA	17.2(0.1)	19.4(0.1)	17.1(1.9)	18.8(1.8)	−0.4(4.2)	−2.1(5.1)
EMF	19.6(0.2)	21.0(0.2)	20.4(1.6)	18.9(2.1)	2.9(4.6)	−7.0(6.4)
EMA	15.4(0.2)	18.5(0.2)	15.0(3.5)	19.5(1.7)	−1.4(3.5)	2.9(5.6)
EMTFA	16.4(0.1)	18.2(0.1)	14.3(0.4)	18.6(0.7)	−7.0(0.4)	1.3(1.0)

[a] Reference 5. [b] $\Delta G^{\ddagger}$ and $\Delta H^{\ddagger}$ in kcal mol^{-1} and $\Delta S^{\ddagger}$ in cal mol^{-1} K^{-1}.

nances is the result of the magnetic anisotropy of the amide group. Previous studies of *N*-substituted oxoamides have shown that the *N*-methyl protons anti to the carbonyl oxygen resonate to lower field than do the syn *N*-methyl protons in formamide, trifluoroacetamide, and acetamide systems.[1−9,14,26] Magnitudes of coupling constants have also provided conformational assignment information. Long-range J_{H-H} and J_{H-F} coupling constants in *N*-methylalkylamides are typically larger when the *N*-methyl group is syn to the carbonyl oxygen in the formamide systems and anti to the carbonyl oxygen in the trifluoroacetamide and acetamide systems.[1,5,6] Investigation of the *N*-methyl resonances in EMSF, EMSTFA, and EMSA reveal that the anti *N*-methyl group resonates to higher field relative to the syn *N*-methyl group. This assignment is based on the magnitudes of the solution phase coupling constants and observation of extra line broadening in the gas sphase spectra attributed to unresolved coupling and is also consistent with expected relative intensity ratios. It has been previously shown that EMF prefers the syn configuration due to steric interaction between the carbonyl group and the more bulky ethyl group and it is reasonable to assume that this preference should be enhanced by substitution with the thiocarbonyl group. The opposite is likely to be true for the acetamide and trifluoroacetamide systems. Studies of EMA and EMTFA report greater preference for the anti configuration due to steric interaction of the ethyl and CH_3 or CF_3 group. Upon thionylation, this preference should diminish as a result of greater sulfur−ethyl steric interaction. The syn/anti chemical shift reversal is observed in both the gas and solution phases. Previous experimental studies of most *N*,*N*-dimethylthioamides also report this reversal of relative chemical shifts.[4,5] However, reports show that this reversal is absent in *N*,*N*-dimethylthioformamide.[14] Computations (B3LYP/6-31++G**//HF/6-311++G**) of the NMR shielding constants for the amide and thioamide systems predict this trend (see Table 4). The computations are meant only as a qualitative comparison

TABLE 4: Calculated (B3LYP/6-311++G//HF/6-311++G**) and Experimental *N*-Methyl Proton Chemical Shifts[a]**

molecule	calculated	experimental
EMF-syn	2.48	2.78[a]
EMF-anti	2.60	2.78[a]
EMSF-syn	2.72	3.17
EMSF-anti	2.80	3.05
EMTFA-syn	2.61	2.94[a]
EMTFA-anti	2.61	3.06[a]
EMSTFA-syn	2.97	3.33
EMSTFA-anti	2.92	3.29
EMA-syn	2.40	2.86[a]
EMA-anti	2.55	2.91[a]
EMSA-syn	2.92	3.44
EMSA-anti	2.67	3.20

[a] Experimental values were measured at 298 K and are referenced to internal gaseous TMS. The calculated values are referenced to the calculated shielding of TMS (31.59 ppm). [b] Reference 5.

due to exclusion of rovibrational corrections. The tabulated values are the average of the isotropic values for the three methyl protons.[27]

The Gibbs free energy differences, ΔG°, and preferred configurations for the thio and oxo amides are compared in Table 2. The experimental gas-phase populations of all three thio systems show a small increase in the syn concentration relative to the corresponding oxoamides. Upon solvation these values increase further. Thioamide ΔG° values are observed to decrease with increasing thiocarbonyl substituent ($CH_3 > CF_3 > H$). Thiocarbonyl substitution of each amide results in decreased ΔG° values relative to the oxoamide analogues.

***N*-Ethyl, *N*-Methylthioformamide.** The slow exchange ^{1}H NMR spectra of gaseous EMSF consist of a triplet ($J = 7.91$ Hz) centered at 1.19 ppm, two *N*-methyl singlet resonances were observed at 3.05 ppm (anti) and 3.17 ppm (syn) with a limiting chemical shift separation of 0.17 ppm ($\Delta\nu$=34.8 Hz in a 7.05 T magnetic field), two methylene quartets centered at 3.64 ppm ($\Delta\nu$=133.2 Hz). Two formyl proton resonances were observed centered at 9.34 ppm. All resonances are referenced to internal gaseous TMS ($\delta = 0.00$ ppm). The limiting chemical shift differences for the methylene and formyl resonances are considerably larger for EMSF compared to EMF.[5] The *N*-methyl resonances of EMF are reported to be isochronic. Exchange-broadened spectra of the *N*-methyl resonances were obtained over a temperature range of 422.6−442.6 K. Line shape analysis of the exchange broadened formyl resonances at several temperatures yielded essentially identical values for the temperature-dependent rate constants. No temperature dependence of the chemical shifts was observed. Figure 2 shows representative experimental and calculated gas-phase exchange-broadened ^{1}H NMR spectra of the *N*-methyl resonances.

Exchange-broadened spectra were also collected for 1 mol % EMSF in decalin. The slow exchange spectra consist of overlapping triplets ($^3J_{H-H}$= 6.21 Hz) centered at 1.24 ppm, two *N*-methyl resonances at 3.19 ppm (anti) and 3.40 ppm (syn) ($\Delta\nu = 63.0$ Hz), two methylene quartets at 3.81 ppm ($\Delta\nu =$ 123 Hz), and two formyl proton resonances at 8.61 ppm, downfield from internal liquid TMS. The lower field *N*-methyl resonance was resolved as a doublet ($^4J_{H-H} = 0.61$ Hz) due to coupling with the formyl proton. Exchange rate data were collected from 433.1 to 444.9 K. The chemical shifts showed temperature dependences to higher field of 0.34(0.05) ppb K^{-1} and 0.41(0.08) ppb K^{-1} for the high and low field *N*-methyl resonances, respectively. The syn and anti methylene slow exchange chemical shifts displayed a temperature dependence

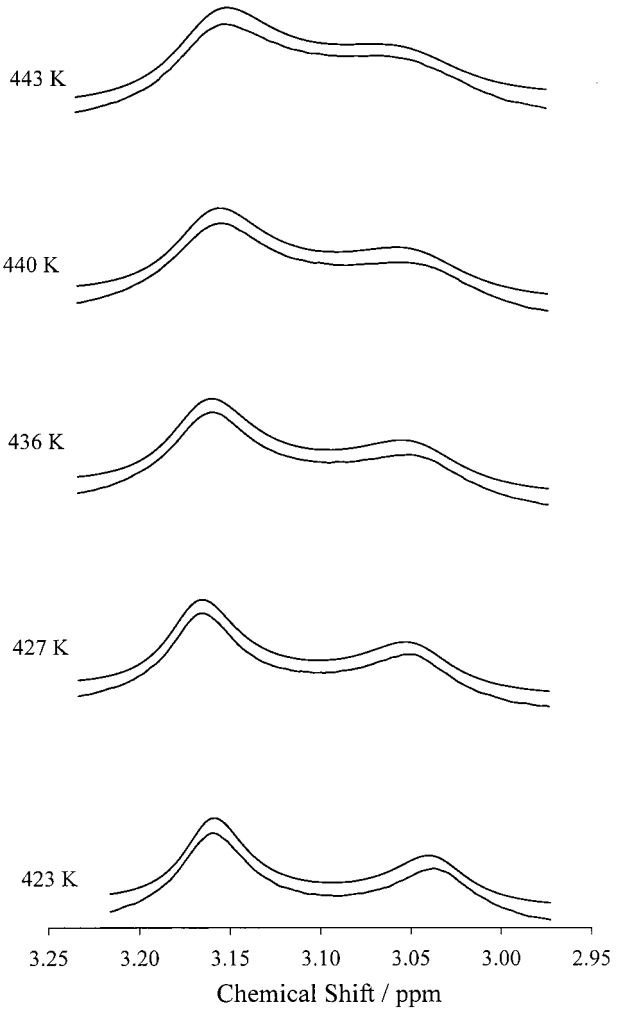

Figure 2. Temperature dependence of the *N*-methyl ^{1}H resonances in gaseous EMSF at 300 MHz. The top and bottom traces correspond to calculated and experimental spectra.

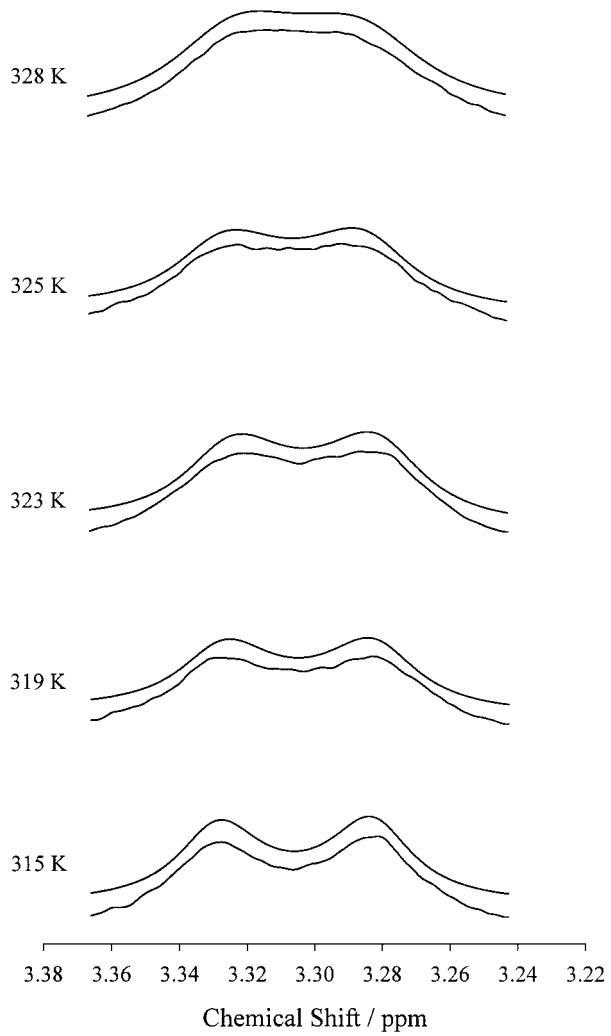

Figure 3. Temperature dependence of the *N*-methyl ^{1}H resonances in gaseous EMSTFA at 300 MHz. The top and bottom traces correspond to calculated and experimental spectra.

of 0.27(0.02) ppb K^{-1}. No temperature dependence of the formyl proton resonance was observed.

***N*-Ethyl, *N*-Methyltrifluorothioacetamide.** The slow exchange ^{1}H NMR spectra of gaseous EMSTFA consist of two overlapping triplets ($^3J_{H-H}$ = 6.71 Hz) at 1.25 ppm, two *N*-methyl resonances at 3.29 ppm (anti) and 3.33 ppm (syn), and two methylene quartets ($^3J_{H-H}$ = 6.71 Hz) centered at 3.89 ppm, downfield from gaseous internal TMS. The higher field *N*-methyl resonance appears broadened due to unresolved coupling with the CF_3 group. The $^5J_{H-F}$ spin−spin coupling constants for the anti conformer are larger due to a large contribution to the coupling from a through space mechanism.[28] Again, no temperature dependence of the chemical shifts was observed. Exchange rate data used for line shape analysis were collected for the *N*-methyl resonances from 315.3 to 328.5 K. Representative experimental and calculated spectra are shown in Figure 3.

Additionally, solution phase spectra of 1 mol % EMSTFA in TClE-d_2 were acquired. The slow exchange spectra consist of two triplets ($^3J_{H-H}$ = 7.33 Hz) centered at 1.27 ppm, anti *N*-methyl quartet ($^5J_{H-F}$ = 1.22 Hz) at 3.34 ppm, syn *N*-methyl singlet at 3.39 ppm, and two methylene quartets ($^3J_{H-H}$ = 7.33 Hz) centered at 3.87 ppm, all referenced to internal liquid TMS. Exchange rate data were acquired from 365.0 to 379.5 K. The fluorine coupling was included in the fitting of these liquid spectra. A small temperature dependence of 0.46(0.08) ppb K^{-1} was observed for the *N*-methyl resonances.

***N*-Ethyl, *N*-Methylthioacetamide.** Slow exchange ^{1}H NMR spectra of gaseous EMSA consist of overlapping ethyl CH_3 resonances at 1.53 ppm, a singlet resonance at 2.88 ppm, two *N*-methyl resonances at 3.20 ppm (anti) and 3.44 ppm (syn), and two methylene-broadened quartet resonances centered at 3.89 ppm. All are referenced to internal gaseous TMS. No temperature dependence of the chemical shifts was observed. Exchange rate data were collected from 347.2 to 364.5 K. Exchange rate data from the *N*-methylene resonances were obtained at several temperatures and found to be in good agreement with results obtained from the *N*-methyl resonances.

Solution phase slow exchange spectra consist of two ethyl CH_3 resonances centered at 1.01 ppm, two overlapping multiplets at 2.35 ppm, anti *N*-methyl resonance at 3.54 ppm, syn *N*-methyl resonance at 3.27 ppm, and two methylene quartet ($^3J_{H-H}$ = 7.21 Hz) resonances at 3.72 and 4.21 ppm. Temperature-dependent spectra used for line shape analysis were obtained from 396.9 to 426.5 K. Temperature dependences to higher field of 0.84(0.10) ppb K^{-1} and 0.76(0.07) ppb K^{-1} were observed for the low and high field *N*-methyl resonances, respectively.

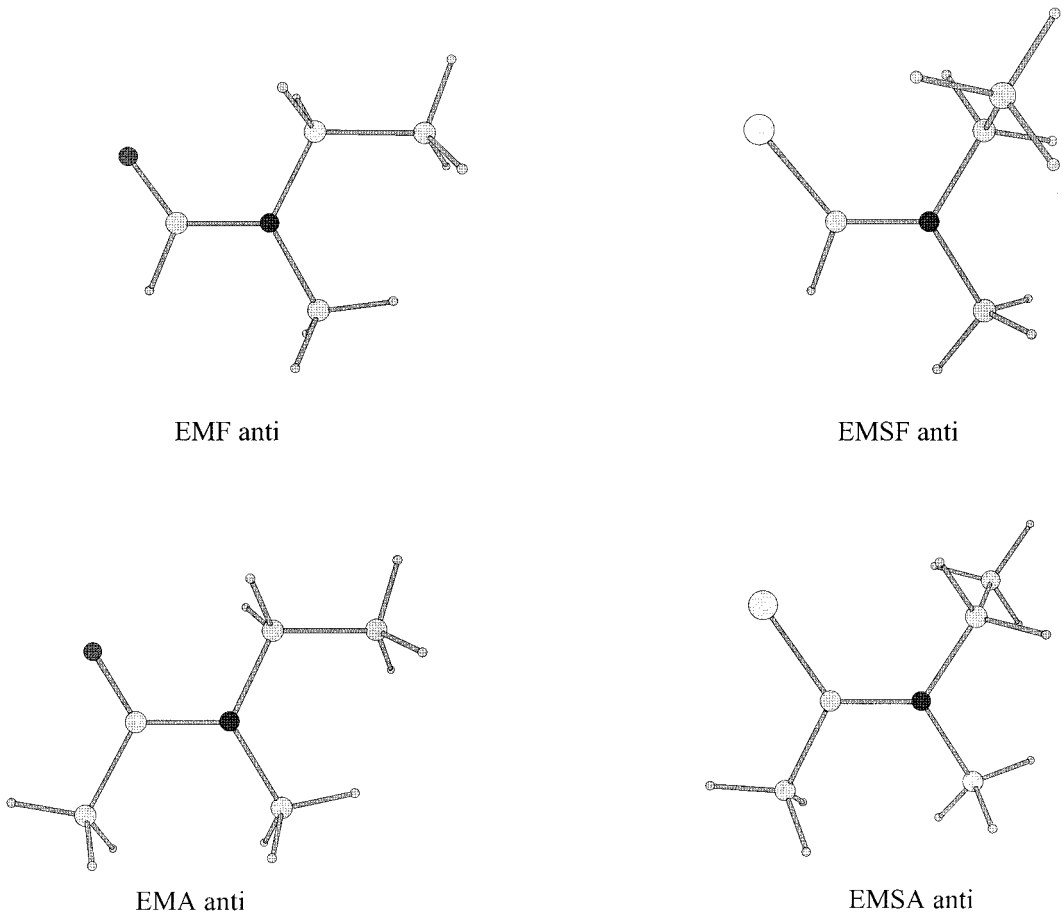

Figure 4. Comparison of the calculated minimum energy configurations (HF/6-311++G**) of the anti conformations of EMF, EMSF, EMA, and EMSA. The torsional angles along the carbonyl carbon−nitrogen−ethyl group carbon atoms are ca. 180° for the oxoamides and 91.0° and 94.3° for EMSF and EMSA, respectively.

Discussion

The gas phase and solution phase kinetic parameters of EMSF, EMSA, and EMSTFA and their corresponding oxoamide analogues are summarized in Table 1. Liquid-phase barriers are higher (1−4 kcal mol^{-1}) than in the gas phase. Substitution with the larger sulfur atom is observed to affect the liquid phase rotational barriers to a greater extent relative to the oxoamide liquid systems. Table 1 shows that the exchange rate constants are considerably lower for the solvated systems, resulting in higher activation barriers. Because the intrinsic effects of structure and reactivity can be obscured by solvent interactions, gas-phase studies are much better suited to investigate kinetic and thermodynamic effects of substituents.

The gas-phase thioamide activation barriers listed in Table 1 are consistently higher than those of the corresponding oxoamide analogues in both gases and liquids. Table 1 shows that increasing the bulk of the thiocarbonyl substituent lowers the rotational barrier. This decrease is attributed to destabilization of the planar ground state due to the inability to accommodate larger substituents in the amide plane. Substitution of H (covalent diameter is 1.2 Å) with CH_3 (3.8 Å) results in a 4.8 kcal mol^{-1} decrease in barrier height.[30] Replacement with CF_3 (4.4 Å) results in a 5.4 kcal mol^{-1} decrease.[30] This trend has been previously observed in both oxoamide and thioamide molecular systems. The extent of destabilization, however, is greater for the thioamides, indicating greater steric sensitivity. Although substituent electronegativity has been shown to affect barrier heights in amides and thioamides, the steric interactions dominate in trifluoroacetamides and trifluorothioacetamides. Comparison of our gas-phase EMSF, EMSA, and EMSTFA activation barriers with values for *N*,*N*-dimethylthioformamide ($\Delta G^{\ddagger} = 22.5(0.1)$ kcal mol^{-1}), *N*,*N*-dimethylthioacetamide ($\Delta G^{\ddagger} = 18.0(0.1)$ kcal mol^{-1}), and *N*,*N*-dimethyltrifluorothioacetamide ($\Delta G^{\ddagger} = 17.2(0.1)$ kcal mol^{-1}) shows essentially no change in barrier height with the *N*-ethyl group substitution.[18] This can be attributed to the ability of the ethyl group to adopt a conformation which minimizes the steric repulsion in the ground state.

Table 2 shows the gas phase and solution phase conformer Gibbs energy differences, $\Delta G°$ ($\Delta G° = G°$ (methyl group syn to thionyl sulfur) − $G°$ (methyl group anti to thionyl sulfur)), for *N*-ethyl, *N*-methylthioamides and *N*-ethyl, *N*-methylamides. All of the differences are small, indicating that the steric requirements of a methyl group and an ethyl group are similar in these molecules. The results do, however, show that EMSF clearly prefers the syn configuration, whereas EMSA and EMSTFA prefer the anti configuration. In comparison to the amide values, the thioamide conformer Gibbs energies are significantly more negative. The gas-phase EMSF $\Delta G°$ is ca. 58% more negative than the corresponding amide value. This large difference in $\Delta G°$ values is the result of increased preference for the syn conformer in the thioamide system. The syn configuration minimizes the sulfur−ethyl group interaction. The EMSA and EMSTFA $\Delta G°$ values are ca. 69% and 53% less positive compared to the amide values, respectively. This indicates a decrease of the preferred anti configuration. As in EMSF, the interaction between the sulfur and the ethyl group is minimized, indicating an increased steric interaction between

the ethyl group and sulfur atom relative to the thiocarbonyl substituent−ethyl group interaction. EMSTFA experiences a smaller decrease of $\Delta G°$ in comparison to EMSA because of the greater steric destabilization of the CF_3 group and the alkyl substituent relative to the CH_3 group.

Minimum energy calculations of the syn and anti configurations were performed for the amide and thioamide systems. The calculated $\Delta G°$ values for these structures are shown in Table 2. The computed values are consistently 25−30% smaller than the experimental values; however, the calculations accurately predict the observed trend. The $\Delta G°$ calculations for the formamide systems favor the syn form by 0.15 kcal mol^{-1} (EMSF) and by 0.12 kcal mol^{-1} (EMF). In contrast, the $\Delta G°$ calculations predict the trifluoroacetamide and acetamide systems to favor the anti form. EMSA and EMA favor the anti form by 0.04 kcal mol^{-1} and 0.13 kcal mol^{-1}, respectively. Similarly, EMSTFA and EMTFA favor the anti form by 0.04 kcal mol^{-1} and 0.14 kcal mol^{-1}. All of the values are significantly smaller than the predicted conformer stability of *N*-methylacetamide. *Ab initio* calculations of $\Delta G°$ predict the anti form to be 2.5 kcal mol^{-1} more stable than the syn form.[7] The full geometry optimization calculations predict significantly different minimum energy ethyl group orientations for oxoamides and thioamides. Figure 4 shows that the minimum energy form of oxoamides, anti-EMF and anti-EMA has all the heavy atoms coplanar with the torsional angle, defined along the carbonyl carbon−nitrogen−ethyl group carbon atoms, ca. 180°. In corresponding thioamides, the minimum energy configuration has the terminal methyl of the ethyl group almost orthogonal to the plane of the other heavy atoms with calculated torsional angles of 94.3° and 91.0° for the anti forms of EMSA and EMSF, respectively. The orientation of the ethyl group is essentially unchanged upon thionylation for anti and syn EMTFA, syn EMA, and syn EMF.

Upon solvation the $\Delta G°$ values decrease for all three thioamide systems, illustrating a stabilizing effect of the syn conformation compared to the anti conformation. The calculated dipole moments tabulated in Table 2 show that the syn conformers are more polar than the anti conformers for the amides and thioamides, indicating that introduction of solvent would stabilize the syn form to a greater extent than the anti form. It is possible that stabilizing solvent interactions are maximized with the thioamides in the syn configuration because the alkyl and the thiocarbonyl groups are more accessible to intermolecular interactions. In the anti conformation, intramolecular thiocarbonyl-alkyl electrostatic interactions can occur, inhibiting interactions with solvent molecules. The same trend has been observed in liquid-phase asymmetric amide systems. However, in these molecules a much greater decrease of $\Delta G°$ is observed relative to the gas phase. The listed gas phase and solution phase $\Delta G°$ values determined from the temperature-dependent population data were limited by sample vapor pressure and could not be separated into entropic and enthalpic contributions.

In conclusion, thionylation of asymmetric amides results in significant changes in internal rotational barriers and conformer relative energy differences. In the past there has been substantial experimental and theoretical work performed to investigate substituent effects in amides; however, no previous data had been available for asymmetric thioamides. The present study shows that solvation significantly affects both $\Delta G^{\ddagger}_{298}$ and $\Delta G°$ values for EMSF, EMSA, and EMSTFA. The gas phase activation barriers for these systems are not significantly different than the values for *N*,*N*-dimethylthioamides, indicating the barrier to rotation is insensitive to *N*-ethyl substitution. The barriers are primarily influenced by the nature of the thiocarbonyl substituent. The conformational equilibria are significantly different for thioamides relative to their oxoamide analogues. Upon thionylation, the $\Delta G°$ values become more negative for all three systems. *Ab initio* calculations predict conformer relative energy differences which are consistently smaller than those observed, but they correctly predict the lower energy conformer in all cases.

Acknowledgment. The authors are pleased to acknowledge the National Science Foundation (CHE 93-21079) and the University of California−Davis Committee on Research for support of this research.

References and Notes

(1) LaPlanche, L. A.; Rogers, M. T. *J. Am. Chem. Soc.* **1963**, *85*, 3728.
(2) LaPlanche, L. A.; Rogers, M. T. *J. Am. Chem. Soc.* **1964**, *86*, 337.
(3) Jackman, L. M.; Cotton, F. A *Dynamic Nuclear Magnetic Resonance Spectroscopy*; Academic Press: New York, 1975; Chapter 7.
(4) Stewart, W. E.; Siddall, T. H., III *Chem. Rev.* **1970**, *70*, 517.
(5) Suarez, C.; Tafazzoli, M.; True, N. S.; Gerrard, S.; LeMaster, C. B.; LeMaster, C. L. *J. Phys. Chem.* **1995**, *99*, 8170.
(6) Taha, A. N.; Neugebauer-Crawford, S. M.; True, N. S. *J. Phys. Chem. A.* **1998**, *102* (8), 1425.
(7) Jorgensen, W. L.; Gao, J. *J. Am. Chem. Soc.* **1988**, *110*, 4212.
(8) Fantoni, A. C.; Caminati, W. *J. Chem. Soc., Faraday Trans.* **1996**, *92* (3), 343.
(9) Glendening, E. D.; Hrabal, J. A. *J. Am. Chem. Soc.* **1997**, *119*, 12940.
(10) Sandstrom, J. *J. Phys. Chem.* **1967**, *71*, 2318.
(11) Wiberg, K. B.; Rablen, P. R. *J. Am. Chem. Soc.* **1995**, *117*, 2201.
(12) Laidig, K. E.; Cameron, L. M. *J. Am. Chem. Soc.* **1996**, *118*, 1737.
(13) Drakenberg, T. *J. Phys. Chem.* **1976**, *80*, 1023.
(14) Neuman, R. C., Jr.; Young, L. B. *J. Phys. Chem.* **1965**, *69*, 1777.
(15) Lauvergnat, D.; Hiberty, P. C. *J. Am. Chem. Soc.* **1997**, *119*, 9478.
(16) Kleinpeter, E. *J. Mol. Struct.* **1996**, *380*, 139.
(17) Kim, W.; Lee, J.-H.; Choi, Y. S.; Choi, J.-H.; Yoon, C.-J. *J. Chem. Soc., Faraday Trans.* **1998**, *94*, 2663.
(18) Neugebauer-Crawford, S. M.; Taha, A. N.; True, N. S.; LeMaster, C. B. *J. Phys. Chem. A.* **1997**, *101*, 4699.
(19) Suarez, C.; LeMaster, C. B.; LeMaster, C. L.; Tafazzoli, M.; True, N. S. *J. Phys. Chem.* **1990**, *94*, 6679.
(20) Wagner, R. B.; Zook, H. D. *Synthetic Organic Chemistry*; Wiley: New York, 1953.
(21) (a) Stephenson, D. S.; Binsch, G. Program No. 365. (b) LeMaster, C. B.; LeMaster, C. L.; True, N. S. Programs No. 569 and QCMP059. Quantum Chemistry Program Exchange, Indiana University, Bloomington, IN 47405.
(22) Frisch, M. J.; Trucks, G. W.; Schlegel, H. B.; Scuseria, G. E.; Robb, M. A.; Cheeseman, J. R.; Zakrzewski, V. G.; Montgomery, J. A., Jr.; Stratmann, R. E.; Burant, J. C.; Dapprich, S.; Millam, J. M.; Daniels, A. D.; Kudin, K. N.; Stain, M. C.; Farkas, O.; Tomasi, J.; Barone, V.; Cossi, M.; Cammi, R.; Mennucci, B.; Pomelli, C.; Adamo, C.; Clifford, S.; Ochterski, J.; Petersson, G. A.; Ayala, P. Y.; Cui, Q.; Morokuma, K.; Malick, D. K.; Rabuck, A. D.; Raghavachari, K.; Foresman, J. B.; Cioslowski, J.; Oritz, J. V.; Stefanov, B. B.; Liu, G.; Liashenko, A.; Piskorz, P.; Komaromi, I.; Gomperts, R.; Martin, R. L.; Fox, D. J.; Keith, T.; Al-Laham, M. A.; Peng, C. Y.; Nanayahhara, A.; Gonsalez, C.; Challacombe, M.; Gill, P. M. W.; Johnson, B.; Chen, W.; Wong, M. W.; Andres, J. L.; Head-Gordon, M.; Replogle, E. S.; Pople, J. A. Gaussian 98 (Revision A.7); Gaussian, Inc.: Pittsburgh, PA 1998.
(23) Curtiss, L. A.; Raghavachari, K.; Trucks, G. W.; Pople, J. A. *J. Chem. Phys.* **1991**, *94*, 7221.
(24) Curtiss, L. A.; Carpenter, J. E.; Raghavachari, K.; Pople, J. A. *J. Chem. Phys.* **1992**, *96*, 9030.
(25) Rablen, P. R.; Pearlman, S. A.; Finkbiner, J. *J. Phys. Chem. A* **1999**, *103*, 7357.
(26) Paulsen, H.; Todt, K. *Angew. Chem., Int. Ed. Engl.* **1966**, *5* (10), 899.
(27) The average of the static values is predicted to be very similar to the dynamic time average due to the similarity of the calculated shift tensors.
(28) Reeves, L. W.; Shaddick, R. C.; Shaw, K. W. *Can. J. Chem.* **1971**, *49*, 3683.
(29) LeMaster, C. B.; True, N. S. *J. Phys. Chem.* **1989**, *93*, 1307.
(30) The values listed are the estimated diameters of the groups using the AM1 Hamiltonian. Program N. 506; Quantum Chemistry Program Exchange, Indiana University, Bloomington, IN 47405.